Bioorganic & Medicinal Chemistry Letters 18 (2008) 5372–5376

Contents lists available at ScienceDirect

Bioorganic & Medicinal Chemistry Letters

journal homepage: www.elsevier.com/locate/bmcl

Identification of novel inhibitors of extracellular signal-regulated kinase 2 based on the structure-based virtual screening

Hwangseo Park [a,*], Young Jae Bahn [b], Dae Gwin Jeong [b], Eui Jeon Woo [b,c], Jung Sun Kwon [b], Seong Eon Ryu [b,*]

[a] Department of Bioscience and Biotechnology, Sejong University, 98 Kunja-Dong, Kwangjin-Ku, Seoul 143-747, Republic of Korea
[b] Systemic Proteomics Research Center, Korea Research Institute of Bioscience and Biotechnology, 52 Eoeun-Dong, Yuseong-Gu, Daejeon 305-333, Republic of Korea
[c] Translational Research Center, Korea Research Institute of Bioscience and Biotechnology, 52 Eoeun-Dong, Yuseong-Gu, Daejeon 305-333, Republic of Korea

ARTICLE INFO

Article history:
Received 30 June 2008
Revised 23 August 2008
Accepted 15 September 2008
Available online 18 September 2008

Keywords:
Virtual screening
Docking
ERK2
Inhibitor
Anticancer agents

ABSTRACT

Extracellular signal-regulated kinase 2 (ERK2) has become an attractive target for the development of therapeutics for the treatment of cancer. We have been able to identify eight new inhibitors of ERK2 by means of a drug design protocol involving the virtual screening with docking simulations and in vitro enzyme assay. The newly discovered inhibitors can be categorized into three structural classes and reveal a significant potency with IC_{50} values ranging from 1 to 30 μM. Therefore, all of the three inhibitor scaffolds deserve further development by structure–activity relationship or de novo design methods. Structural features relevant to the stabilizations of the newly identified inhibitors in the ATP-binding site of ERK2 are discussed in detail.

The extracellular signal-regulated kinases (ERKs) are involved in the Ras/Raf/MEK/ERK signal transduction pathway whose activation is a common feature of many deregulated molecular lesions in cancer. Indeed, a constitutive activation of this pathway has proven to cause the proliferation of many human cancers in lung, colon, pancreas, kidney, and ovary.[1–5] The reason for the involvement of the pathway in cancer lies in its role in controlling a variety of fundamental cellular processes including cell survival, proliferation, motility, and differentiation. The Ras/Raf/MEK/ERK signal transduction pathway can also serve as an intracellular mediator in signaling aberrations in many inflammatory processes.[6,7] Therefore, this pathway represents an attractive target for pharmacological invention in cancer and inflammatory diseases.

ERK acts as a central point where multiple signaling pathways coalesce to drive transcription and thus plays a pivotal role in downstreaming the pathways. There are two isoforms of ERK proteins (ERK1 and ERK2) that are linked to the proliferation and survival of cancer cells.[8] The two isoform ERKs share 88% sequence identity with the conservation of the residues in the ATP-binding site. X-ray crystallographic data showed that ERK2 is a proline-directed kinase whose phosphorylation site is similar in structure to that of cyclin-dependent kinase 2 (CDK2).[9] The X-ray crystal structures of ERK2 in complex with selective inhibitors were also reported.[10–12] The presence of structural information about the nature of the interactions between ERK2 and small molecule inhibitors has made it a plausible task to design a good lead compound for anticancer drugs. Indeed, several ATP-independent inhibitors have been discovered by means of in silico screening with docking simulations of a variety of small molecules in the active site of ERK2.[13]

Nonetheless, discovery of ERK2 inhibitors has lagged behind the pharmacological and structural studies. Only a few structural classes of ERK2 inhibitors have been reported so far. Several derivatives of 5-pyrazolo[1,5-*a*]pyridin-3-yl-1*H*-pyrazolo[3,4-*c*]pyridazine scaffold proved to be competitive and selective inhibitors of ERK1 and ERK2 with micromolar and submicromolar inhibitory activity.[10,11] Recently, various pyrazolylpyrrole derivatives have also been identified as potent selective inhibitors of ERK2 with multiple binding modes.[12] A few micromolar inhibitors have also been discovered with a structure-based virtual screening approach.[13]

In this study, we identify the novel classes of ERK2 inhibitors by means of a structure-based drug design protocol involving the virtual screening with docking simulations and in vitro enzyme assay. The characteristic feature that discriminates our virtual screening approach from the others lies in the implementation of an accurate solvation model in calculating the binding free energy between ERK2 and putative ligands, which would have an effect of increasing the hit rate in enzyme assay.[14] It will be shown that the docking simulation with the improved binding free energy function can

* Corresponding authors. Tel.: +82 2 3408 3766; fax: +82 2 3408 4334 (H.P.), tel.: +82 42 860 4149; fax: +82 42 860 4598 (S.E.R.).
E-mail addresses: hspark@sejong.ac.kr (H. Park), ryuse@kribb.re.kr (S.E. Ryu).

0960-894X/$ - see front matter © 2008 Elsevier Ltd. All rights reserved.
doi:10.1016/j.bmcl.2008.09.058

be a useful tool for elucidating the activities of the identified inhibitors, as well as for enriching the chemical library with molecules that are likely to have desired biological activities.

The 3-D coordinates in the X-ray crystal structure of ERK2 in complex with the inhibitor FR180204 (PDB code: 1TVO)[10] were selected as the receptor model in the virtual screening with docking simulations. After removing the ligand and solvent molecules, hydrogen atoms were added to each protein atom. A special attention was paid to assign the protonation states of the ionizable Asp, Glu, His, and Lys residues in the X-ray structure of ERK2. The side chains of Asp and Glu residues were assumed to be neutral if one of their carboxylate oxygens pointed toward a hydrogen-bond accepting group including the backbone aminocarbonyl oxygen at a distance within 3.5 Å, a generally accepted distance limit for a hydrogen bond of moderate strength.[15] Similarly, the lysine side chains were assumed to be protonated unless the NZ atom was in proximity of a hydrogen-bond donating group. The same procedure was also applied to determine the protonation states of ND and NE atoms in His residues.

The docking library for ERK2 comprising about 85,000 compounds was constructed from the latest version of the chemical database distributed by Interbioscreen (http://www.ibscreen.com) containing approximately 30,000 natural and 320,000 synthetic compounds. The selection was based on the drug-like filters that adopt only the compounds with physicochemical properties of potential drug candidates[16] and without reactive functional group(s). All of the compounds included in the docking library were then subjected to the Corina program to generate their 3-D atomic coordinates, followed by the assignment of Gasteiger–Marsilli atomic charges.[17] We used the AutoDock program[18] in the virtual screening of ERK2 inhibitors because the outperformance of its scoring function over those of the others had been shown in several target proteins.[19] AMBER force field parameters were assigned for calculating the van der Waals interactions and the internal energy of a ligand as implemented in the AutoDock program. Docking simulations with AutoDock were then carried out in the ATP-binding site of ERK2 to score and rank the compounds in the docking library according to their calculated binding affinities.

In the actual docking simulation of the compounds in the docking library, we used the empirical AutoDock scoring function improved by the implementation of a new solvation model for a compound. The modified scoring function has the following form:

$$\begin{aligned}\Delta G_{\text{bind}}^{\text{aq}} = {} & W_{\text{vdW}} \sum_{i=1} \sum_{j>i} \left(\frac{A_{ij}}{r_{ij}^{12}} - \frac{B_{ij}}{r_{ij}^{6}} \right) + W_{\text{hbond}} \sum_{i=1} \sum_{j>i} E(t) \left(\frac{C_{ij}}{r_{ij}^{12}} - \frac{D_{ij}}{r_{ij}^{10}} \right) \\ & + W_{\text{elec}} \sum_{i=1} \sum_{j>i} \frac{q_i q_j}{\varepsilon(r_{ij}) r_{ij}} + W_{\text{tor}} N_{\text{tor}} \\ & + W_{\text{sol}} \sum_{i=1} S_i \left(\text{Occ}_i^{\max} - \sum_{j>i} V_j e^{-\frac{r_{ij}^2}{2\sigma^2}} \right)\end{aligned} \quad , \quad (1)$$

where W_{vdW}, W_{hbond}, W_{elec}, W_{tor}, and W_{sol} are the weighting factors of van der Waals, hydrogen bond, electrostatic interactions, torsional term, and desolvation energy of inhibitors, respectively. r_{ij} represents the interatomic distance, and A_{ij}, B_{ij}, C_{ij}, and D_{ij} are related to the depths of the potential energy well and the equilibrium separations between the two atoms. The hydrogen bond term has an additional weighting factor, $E(t)$, representing the angle-dependent directionality. Cubic equation approach was applied to obtain the dielectric constant required in computing the interatomic electrostatic interactions between ERK2 and a ligand molecule.[20] In the entropic term, N_{tor} is the number of sp^3 bonds in the ligand. In the desolvation term, S_i and V_i are the solvation parameter and the fragmental volume of atom i,[21] respectively, while $\text{Occ}_i^{\max}$ stands for the maximum atomic occupancy. In the calculation of molecular solvation free energy term in Eq. 1, we used the atomic parameters recently developed by Kang et al.[22] because those of the atoms other than carbon were unavailable in the current version of AutoDock. This modification of the solvation free energy term is expected to increase the accuracy in virtual screening because the underestimation of ligand solvation often leads to the overestimation of the binding affinity of a ligand with many polar atoms.[14]

To obtain better binding configurations for ERK2-inhibitor complexes, we have performed molecular dynamics (MD) in aqueous solution. The most stable structures of ERK2-inhibitor complexes obtained from docking simulation were equilibrated in solution through 0.5 ns MD simulation with AMBER program, which had been successful in modeling the structures of proteins[23] and nucleic acids[24] in solution. This equilibration procedure started with the addition sodium ions as the counterion to neutralize the total charge of the all-atom model of ERK2. The system was then immersed in a rectangular solvent box containing about 8000 TIP3P water molecules. After 1000 cycles of energy minimization to remove bad van der Waals contacts, we equilibrated the system beginning with 20 ps equilibration dynamics of the solvent molecules at 300 K. The next step involved equilibration of the solute with a fixed configuration of the solvent molecules for 10 ps at 10, 50, 100, 150, 200, 250, and 300 K. Then, the equilibration dynamics of the entire system was performed at 300 K for 500 ps using the periodic boundary condition. The SHAKE algorithm[25] was applied to fix all bond lengths involving hydrogen atom. We used a time step of 1.5 fs and a nonbond-interaction cutoff radius of 12 Å.

Of the 85,000 compounds subject to the virtual screening with docking simulations, 150 top-scored compounds were selected as virtual hits. One hundred and forty-eight of them were available from the compound supplier and were tested for inhibitory activity against ERK2 by in vitro enzyme assay.[28] As a result, we identified 23 compounds that inhibited the catalytic activity of ERK2 by more than 50% at the concentration of 50 μM. Among them, eight compounds revealed a high potency with more than 70% inhibition at the same concentration and were selected to determine IC_{50} values. The chemical structures and the inhibitory activities of the newly identified inhibitors are shown in Figure 1 and Table 1, respectively. The structures of the remaining 15 compounds revealing more than 50% inhibition of ERK2 activity at 50 μM are shown in Supplementary information. We note that the compounds **1**, **2**, and **3** share a common 3-benzyl-5-methylene-2-thioxo-thiazolidin-4-one scaffold. In this inhibitor scaffold, the derivation of a hydrophobic group at the end of molecular structure seems to have a negative effect on the inhibitory activity. Compounds **4**, **5**, and **6** possess the *N*-(5-amino-1-phenyl-1*H*-[1,2,4]triazole-3-yl)-benzamide group as a common scaffold. Compounds **7** and **8** are structurally very similar with the common 5-benzyloxy-2-(4-phenyl-1*H*-pyrazol-3-yl)-phenol scaffold and have moderate inhibitory activities with the IC_{50} values of 15–30 μM. The eight inhibitors shown in Figure 1 can thus be divided into three structural classes. To the best of our knowledge, these compounds have not been reported as ERK inhibitors so far. Therefore, all of the three inhibitor scaffolds deserve further development by structure–activity relationship (SAR) or de novo design methods.

Since the selectivity for ERK2 against other MAP kinases has been the most important issue in the development of ERK2 inhibitors, we have compared the inhibitory activities of **1**, **4**, and **7** for ERK2 and p38α protein. These inhibition assays for selectivity were done in duplicates at the concentration of 100 μM. As can be seen in Table 2, all three compounds reveal approximately 90% inhibition for ERK2 at the concentration of 100 μM whereas the catalytic activities of p38α are reduced by no more than 25% at the same concentration of inhibitors. Considering the structural similarity between ERK and p38 protein, the inhibitors found in this study seem to bind in novel way in the ATP-binding site of ERK2.

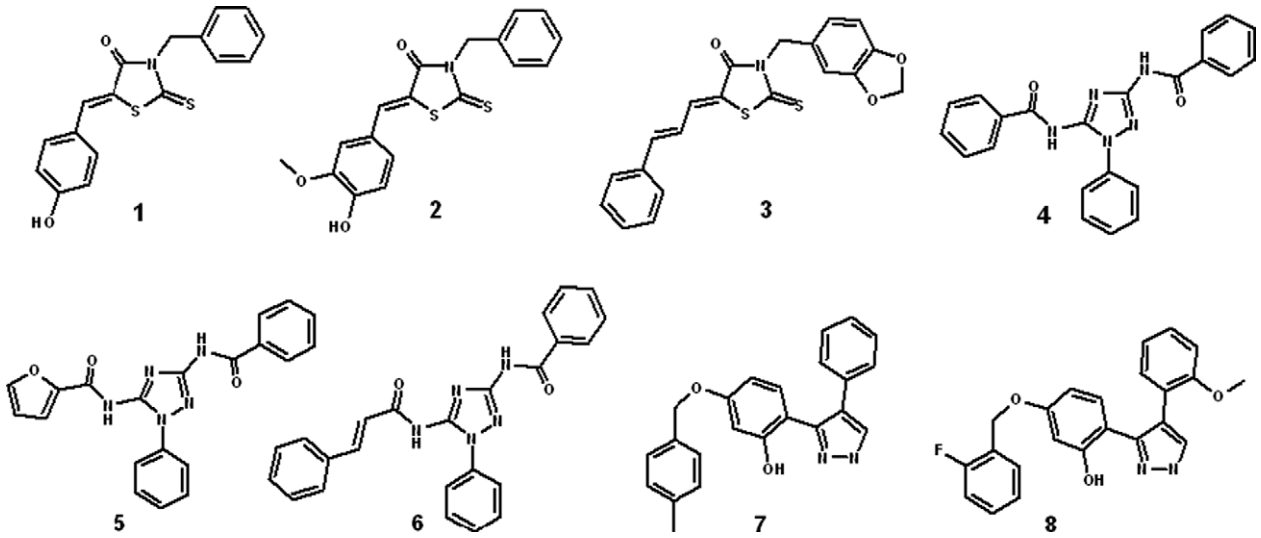

Figure 1. Chemical structures of the newly identified ERK2 inhibitors.

Table 1
IC_{50} values (in μM) of the reference and compounds **1**–**8** against ERK2

Compound	IC_{50} (μM)	Compound	IC_{50} (μM)
SB220025	19.0	**5**	18.3
1	5.5	**6**	25.6
2	14.3	**7**	16.9
3	23.7	**8**	27.4
4	8.3		

Table 2
Comparison of the inhibitory activities of **1**, **4**, and **7** for ERK2 and p38 protein

Compound	% Inhibition at 100 μM for ERK2	% Inhibition at 100 μM for p38α
1	92.7 ± 6.1	16.7 ± 4.4
4	93.1 ± 5.8	24.5 ± 5.3
7	87.9 ± 8.6	12.3 ± 3.9

To obtain structural insight into the inhibitory mechanisms of the identified inhibitors of ERK2, their binding modes in the ATP-binding site were investigated in comparison with that of the known inhibitor SB220025. Figure 2 shows the best-scored AutoDock conformations of SB220025, **1**, and **4** in the ATP-binding site gorge of ERK2. As revealed by the superposition of the docked structures, all of the inhibitors seem to be stabilized in the ATP-binding site due in part to the interactions with the two catalytic residues, Lys54 and Asp167. It is also a common feature in binding modes that one of the terminal groups of the inhibitors resides in a close proximity of the gatekeeper site, the interaction with which can serve as a filter to screen the selective kinase inhibitors.[26] In order to examine the possibility of the allosteric inhibition of ERK2 by the identified inhibitors, docking simulations were carried out with the grid maps for the receptor model so as to include the entire part of ERK2. However, the binding configuration in which an inhibitor resides outside the ATP-binding site was observed neither for the new inhibitors nor for SB220025. These results support the possibility that the inhibitors would impair the catalytic activity of ERK2 through the specific binding in the ATP-binding site.

To obtain an improved binding configuration of ERK2-**1** complex, we have carried out MD simulations of the complex in aqueous solution as described above. The representative MD trajectory

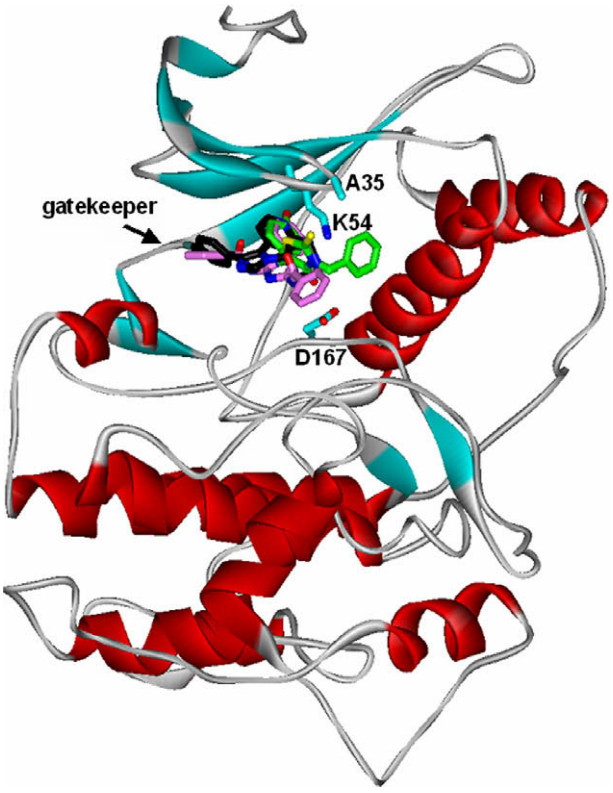

Figure 2. Comparative view of the binding modes of SB220025, **1**, and **4** in the ATP-binding site of ERK2. Carbon atoms of the amino acid residues of ERK2, SB220025, **1**, and **4** are indicated in cyan, black, green, and pink, respectively.

snapshot for the complex is shown in Figure 3. It is noted that the carbonyl oxygen of the inhibitor receives a hydrogen bond from the side chain Lys54. This structural feature is consistent with the X-ray crystallographic data indicating a pivotal role of Lys54 in accommodating a ligand in the ATP-binding site of ERK2.[10–12] A stable hydrogen bond is also established between the phenolic group of the inhibitor and the backbone aminocarbonyl oxygen of Ile103. This hydrogen bond can serve as a clue for designing the selective ERK2 inhibitors since Ile103 resides in the gatekeeper

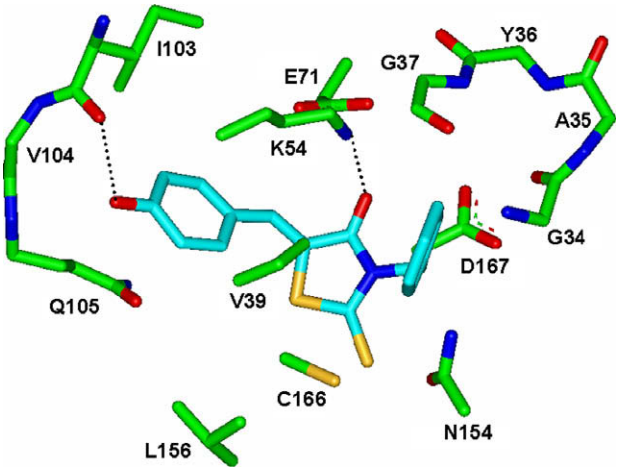

Figure 3. Representative MD trajectory snapshot of ERK2-**1** complex. Carbon atoms of the protein and the ligand are indicated in green and cyan, respectively. Each dotted line indicates a hydrogen bond.

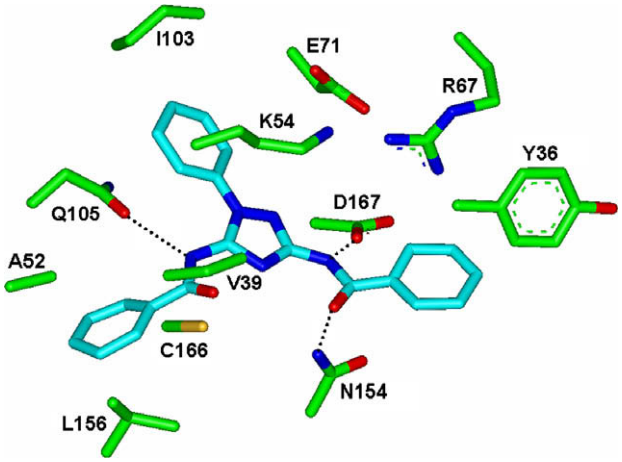

Figure 4. Representative MD trajectory snapshot of ERK2-**4** complex. Carbon atoms of the protein and the ligand are indicated in green and cyan, respectively. Each dotted line indicates a hydrogen bond.

site that has been known as a key determinant for kinase inhibitor selectivity.[26] As can be deduced from the decrease in inhibitory activity in going from **1** to **2** and **3** (see Fig. 1 and Table 1), a hydrogen-bonding group seems to be more efficient for inhibitor binding in the gatekeeper site than hydrophobic groups. The inhibitor **1** can be further stabilized in the ATP-binding site by the hydrophobic interactions of its nonpolor groups with the side chains of Val39, Lys54, Leu156, and Cys166. Judging from the overall structural features of the ERK2-**1** complex derived from docking simulations, the inhibitory activity of **1** is likely to stem from the multiple hydrogen bonds and hydrophobic interactions established simultaneously in the ATP-binding site.

We now turn to address the possibility that the inhibitor **1** would form a covalent bond with the side chain of Cys166 in the ATP-binding site. As shown in Figure 3, the thiolate group of Cys166 points toward the side chains of Asn154 and Leu156 instead of the α,β-unsaturated carbonyl moiety of **1**. Furthermore, the SG atom Cys166 stays away from carbonyl and β carbon atoms of **1** at a distance longer than 5.5 Å. Therefore, it seems to be difficult for the covalent bond between Cys166 and the inhibitor to be formed in the ERK2-**1** complex.

Figure 4 shows the representative MD trajectory snapshot for ERK2-**4** complex in aqueous solution. The binding mode of **4** differs from that of **1** in that neither the side chain of Lys54 nor a backbone gatekeeper group is involved in the hydrogen-bond interactions with the inhibitor. In ERK2-**4** complex, however, the side chains of Gln105, Asn154, and Asp167 form three hydrogen bonds with the two amide groups of **4**. Hydrophobic interactions should also be a significant binding force for stabilizing **4** in the ATP-binding site of ERK2 because three phenyl rings of **4** form van der Waals contacts with the side chains of Tyr36, Val39, Ala52, Lys54, and Ile103. We note that one of the phenyl rings of **4** is stabilized in the gatekeeper site through the hydrophobic interaction with the side chain of Ile103, as compared to a corresponding hydrogen bond in the ERK2-**1** complex. The loss of the hydrogen bond with a gatekeeper residue seems not to be compensated by the increase in the number of the other hydrogen bonds and the strengthening of the hydrophobic interactions, which can be an explanation for a little lower inhibitory activity of **4** than **1**.

In summary, we have identified eight new novel inhibitors of ERK2 by applying a computer-aided drug design protocol involving the structure-based virtual screening with docking simulations under consideration of the effects of ligand solvation in the scoring function. These inhibitors can be categorized into three inhibitor scaffolds and reveal a significant potency with IC_{50} values ranging from 1 to 30 μM. Therefore, each of the newly discovered inhibitor scaffolds can deserve further development by structure–activity relationship studies or de novo design methods. Detailed binding mode analyses with docking simulation show that the inhibitors can be stabilized in the ATP-binding site by the simultaneous establishment of multiple hydrogen bonds and van der Waals contacts.

Acknowledgment

This work was supported by the grant from KRIBB Research Initiative Program.

Supplementary data

Supplementary data associated with this article can be found, in the online version, at doi:10.1016/j.bmcl.2008.09.058.

References and notes

1. Sebolt-Leopold, J. S.; Herrera, R. *Nat. Rev. Cancer* **2004**, *4*, 937.
2. Smalley, K. S. *Int. J. Cancer* **2003**, *104*, 527.
3. Kohno, M.; Pouyssegur, J. *Prog. Cell Cycle Res.* **2003**, *5*, 219.
4. Chang, F.; Steelman, L. S.; Shelton, J. G.; Lee, J. T.; Navolanic, P. M.; Blalock, W. L.; Franklin, R.; McCubrey, J. A. *Int. J. Oncol.* **2003**, *22*, 469.
5. Hilger, R. A.; Scheulen, M. E.; Strumberg, D. *Onkologie* **2002**, *25*, 511.
6. Herrera, R.; Sebolt-Leopold, J. S. *Trends Mol. Med.* **2002**, *8*, S27.
7. Kyriakis, J. M.; Avruch, J. *Physiol. Rev.* **2002**, *81*, 807.
8. Lefloch, R.; Pouyssegur, J.; Lenormand, P. *Mol. Cell. Biol.* **2008**, *28*, 511.
9. Canagarajah, B. J.; Khokhlatchev, A.; Cobb, M. H.; Goldsmith, E. J. *Cell* **1997**, *90*, 859.
10. Ohori, M.; Kinoshita, T.; Okubo, M.; Sato, K.; Yamazaki, A.; Arakawa, H.; Nishimura, S.; Inamura, N.; Nakajima, H.; Neya, M.; Miyake, H.; Fujii, T. *Biochem. Biophys. Res. Commun.* **2005**, *336*, 357.
11. Kinoshita, T.; Warizaya, M.; Ohori, M.; Sato, K.; Neya, M.; Fujii, T. *Bioorg. Med. Chem. Lett.* **2006**, *16*, 55.
12. Aronov, A. M.; Baker, C.; Bemis, G. W.; Cao, J.; Chen, G.; Ford, P. J.; Germann, U. A.; Green, J.; Hale, M. R.; Jacobs, M.; Janetka, J. W.; Maltais, F.; Martinez-Botella, G.; Namchuk, M. N.; Straub, J.; Tang, Q.; Xie, X. *J. Med. Chem.* **2007**, *50*, 1280.
13. Chen, F.; Hancock, C. N.; Macias, A. T.; Joh, J.; Still, K.; Zhong, S.; MacKerell, A. D., Jr.; Shapiro, P. *Bioorg. Med. Chem. Lett.* **2006**, *16*, 6281.
14. Shoichet, B. K.; Leach, A. R.; Kuntz, I. D. *Proteins* **1999**, *34*, 4.
15. Jeffrey, G. A. *An Introduction to Hydrogen Bonding*; Oxford University Press: Oxford, 1997.
16. Lipinski, C. A.; Lombardo, F.; Dominy, B. W.; Feeney, P. J. *Adv. Drug Deliv. Rev.* **1997**, *23*, 3.
17. Gasteiger, J.; Marsili, M. *Tetrahedron* **1980**, *36*, 3219.
18. Morris, G. M.; Goodsell, D. S.; Halliday, R. S.; Huey, R.; Hart, W. E.; Belew, R. K.; Olson, A. J. *J. Comput. Chem.* **1998**, *19*, 1639.
19. Park, H.; Lee, J.; Lee, S. *Proteins* **2006**, *65*, 549.

20. Park, H.; Jeon, J. H. *Phys. Rev. E* **2007**, *75*, 021916.
21. Stouten, P. F. W.; Frömmel, C.; Nakamura, H.; Sander, C. *Mol. Simul.* **1993**, *10*, 97.
22. Kang, H.; Choi, H.; Park, H. *J. Chem. Inf. Model.* **2007**, *47*, 509.
23. Case, D. A.; Cheatham, T. E., III; Darden, T.; Gohlke, H.; Luo, R.; Merz, K. M., Jr.; Onufriev, A.; Simmerling, C.; Wang, B.; Woods, R. J. *J. Comput. Chem.* **2005**, *26*, 1668.
24. Park, H.; Lee, S. *J. Chem. Theory Comput.* **2006**, *2*, 858.
25. Ryckaert, J. P.; Ciccotti, G.; Berendsen, H. C. *J. Comput. Phys.* **1977**, *23*, 327.
26. Cohen, M. S.; Zhang, C.; Shokat, K. M.; Taunton, J. *Science* **2005**, *308*, 1318.
27. Wang, Z.; Canagarajah, B. J.; Boehm, J. C.; Kassisà, S.; Cobb, M. H.; Young, P. R.; Abdel-Meguid, S.; Adams, J. L.; Goldsmith, E. J. *Structure* **1998**, *6*, 1117.
28. ERK assay was carried out based on the procedure suggested by Ohori et al.[10] At first bovine myelin basic protein (MBP) solution was diluted with phosphate-buffered saline (PBS) and then coated in each well (1 μg/well) of Nunc-Immuno 96 microwell plates (MaxiSorp™). After washing the plates with 300 μl PBST (PBS containing 0.05% Tween 20), 100 μl blocking buffer (PBST containing 3% bovine serum albumin) was added to each well, which was followed by the incubation of the plates for 1 h at room temperature. The test compounds selected from virtual screening, magnesium/ATP cocktail substrate, and recombinant ERK2 were diluted in assay dilution buffer I with pH 7.2 comprising 20 mM 4-morpholinepropanesulfonic acid (MOPS), 25 mM β-glycerol phosphate, 5 mM ethyleneglycol-bis(2-aminoethylether)-*N*,*N*,*N*′,*N*′-tetraacetic acid (EGTA), 1 mM Na_3VO_4, 1 mM dithiothreitol (DTT), and 0.005% bovine serum albumin. This diluted mixture was then added to each well of the plates. Kinase-withdrawal groups, vehicle groups, and the positive control SB220055 were used for the inter-plate control and background level determination. After incubating for 1 h at room temperature, primary anti-phospho-MBP antibody was diluted to an appropriate concentration with blocking buffer (1:20,000 v/v). This diluted antibody was then transferred to each well of the plates, followed by the addition of the secondary anti-mouse HRP-conjugated polyclonal antibody diluted with blocking buffer (1:5000 v/v). *o*-Phenylenediamine dihydrochloride (OPD) substrate mixture solution was then added to each well and the plates were incubated for 10 min. The enzymatic reaction was stopped by 2.5 M sulfuric acid, and HRP activity was measured at 490 nm. Used as a reference was the known inhibitor SB220055 that has the IC_{50} value of 18 μM against ERK2[27].